Further Studies of the Optimization of a Hurricane Track Prediction Model Using the Adjoint Equations

ROBERT W. JONES

Hurricane Research Division, NOAA/AOML, Miami, Florida

MARK DEMARIA

Tropical Prediction Center, Miami, Florida

(Manuscript received 17 January 1998, in final form 15 June 1998)

ABSTRACT

The method of model fitting, or *adjoint method,* is applied to a barotropic hurricane track forecast model described by DeMaria and Jones using a large sample of forecast cases. The sample includes all Atlantic tropical cyclones that reached hurricane intensity during the 1989–93 hurricane seasons (141 72-h forecasts of 17 storms). The cases considered by DeMaria and Jones are a subset of the present sample. Model-fitting calculations using strong, weak, strong followed by weak, or weak followed by strong model constraints are discussed for data assimilation periods varying from 6 to 72 h. Generally, the best track forecasts occur for shorter assimilation periods and for weak constraints, although only the 12-h assimilation with the weak constraint has less track error than the control forecast without assimilation, and only for the 12-h forecast. The principle reason for this lack of improvement is that the fit of the model to the observed track is good at the middle of the assimilation period, but not very good at the end where the forecast begins. When a future track position at 6 h is included in the assimilation, in order to improve the track fit at the synoptic data time, the resulting track errors average about 10% smaller than the control forecast. The control forecast may also be improved in the same way. In that case, the best assimilation forecasts have 2.5% smaller track errors than the modified control forecasts.

1. Introduction

Accurate numerical hurricane track forecasts are very difficult, because of the lack of data over the tropical oceans. Four-dimensional data assimilation techniques can partially compensate for the lack of spatial data coverage by including observations over an extended time interval. Two recent hurricane tracking studies have adopted this approach for a model based upon the barotropic vorticity equation. Bennett et al. (1993) used a generalized inverse method for tracking 10 cases of Pacific typhoons from the 1990 season. For the 1989 Atlantic hurricane season, DeMaria and Jones (1993, hereafter DJ93) applied the method of model fitting (also known as the *adjoint method*) to track 69 cases from five hurricanes (Dean, Erin, Felix, Gabrielle, and Hugo). Both studies include a means for inserting a vortex by use of synthetic observations. Bennett et al. (1993) reported improvement through the end of their 48-h experiments compared with forecasts made without data assimilation. For DJ93, improved track forecasts were obtained through 60 h for their best assimilation strategy for Hurricane Hugo (18 cases), through 48 h for Hurricane Dean (12 cases), and through 72 h for Hurricane Felix (9 cases). However, track forecasts for Hurricane Erin (8 cases) were not improved and forecasts for Hurricane Gabrielle (22 cases) showed improvement only at 12 h. The Erin forecasts were adversely affected by large initial position errors. The Gabrielle forecasts were adversely affected by failure to completely remove incorrectly positioned vortices from first guess fields before the synthetic vortices were added to the analysis fields. These studies indicate that hurricane track prediction can be improved by implementing four-dimensional data assimilation. However, the results are not conclusive, because there are only 10 cases in Bennett et al. (1993) and difficulties with some of the initial analyses in DJ93.

In this study the method of model fitting of DJ93 is applied to 226 cases from 1989 to 1993. The analyses described in DJ93 have been modified to mitigate the problem of incorrectly positioned vortices. With this large data sample, various assimilation strategies can be meaningfully compared. Both the length of the assimilation period and the number of datasets in the period

Corresponding author address: Dr. Robert W. Jones, Hurricane Research Division, NOAA/AOML, 4301 Rickenbacker Causeway, Miami, FL 33149.
E-mail: robert.w.jones@noaa.gov

will be tested. The strong constraint for assimilations, where the prediction model is exactly satisfied will be compared with the weak constraint where the prediction model is approximately satisfied. As a means of improving the fit of the model track to the observed track at the last synoptic time (usual end of the assimilation), use of future track positions is explored.

The barotropic prediction model and the data assimilation procedures are described in section 2. In section 3, the new datasets are described. In section 4, results from Hurricane Hugo 1989 are presented that contrast the track forecasts made with the old and present datasets. Section 5 summarizes the track forecasts for the entire dataset and for various assimilation strategies. Section 6 discusses the inclusion of track data from the future into either the assimilation or the control forecasts. The use of *future* track positions has application to track models that obtain initial analyses from previous global model forecasts but include current storm positions for generation of synthetic vortex observations.

2. Data assimilation model

The tropical cyclone track forecast model used in this study is governed by the balanced barotropic vorticity equation on a Mercator projection, which can be written as

$$\frac{\partial P}{\partial t} + m\left(u\frac{\partial P}{\partial x} + v\frac{\partial P}{\partial y}\right) + \beta v = \lambda m^2\nabla^2 P + \Phi, \quad (2.1)$$

where

$$P = (m^2\nabla^2 - \gamma^2)\psi, \quad (2.2)$$

$$u = -m\frac{\partial \psi}{\partial y}, \quad (2.3a)$$

$$v = m\frac{\partial \psi}{\partial x}, \quad (2.3b)$$

$$\beta = \frac{2\Omega\cos\theta}{a}, \quad (2.4)$$

and

$$m = \frac{\cos\theta_0}{\cos\theta}. \quad (2.5)$$

In (2.1)–(2.5), P is the potential vorticity, ψ is the streamfunction, m is the map factor, θ is the latitude, θ_0 is the reference or true latitude of the Mercator projection, a is the earth's radius, Ω is the earth's angular speed, λ is the horizontal diffusion coefficient, γ is the inverse of the Rossby radius of deformation (assumed constant), and $\Phi(x, y, t)$ is a specified forcing term. The other variables have their usual meaning. Further details of the model are given in DJ93, although aspects relevant to the current study are described below.

The two parameters in the model are the horizontal diffusion coefficient λ (10^4 m^2 s^{-1}) and the Rossby radius of deformation $1/\gamma$ (800 km). The track forecasts are not sensitive to λ, but are very sensitive to the Rossby radius. The latter is due to the sensitivity of the long Rossby wave phase speeds to this radius in our barotropic model (Cressman 1958). This sensitivity is manifest by excessive retrogression of the subtropical ridge for large Rossby radii (nondivergent) for some hurricane situations. For example, the landfall point in a 72-h forecast of Hurricane Hugo was near Charleston, South Carolina, with a Rossby radius of 800 km, compared with a landfall point near Miami, Florida, when $\gamma = 0$.

To accomodate the larger dataset, the model grid was expanded from 96 × 80 to 256 × 160 intervals with an accompanying change of mesh size from 100 to 50 km. The mesh interval change overcomes computational dispersion that appears in the average track speed for the first 12 h of the control experiment, which are 4.8 and 4.4 m s^{-1} for the 50- and 100-km meshes, respectively. The time step is also adjusted to 300 s from 600 s. The reference latitude was increased from 20° to 30°N.

The integration domain is 3200 km larger in the x direction than in DJ93 and is centered about 20° west of the initial center of each storm, but no farther west than 75°W. With the expanded domain, the west boundary is nearly always west of the Rocky Mountains, which overcomes a Courant–Friedrichs–Levy (CFL) numerical instability that occasionally occurred along the northern grid boundary, when the streamfunction and inflow vorticity are held fixed (as they are for control forecasts without data assimilation and the forecast portion of a data assimilation experiment). The CFL problem is triggered when the domain boundary is close to the relatively large amplitude disturbances in the westerlies over the mountains, which leads to unrealistically large streamfunction gradients. The increased reference latitude also mitigates the CFL problem by slightly reducing the maximum value of the map factor m.

The forecast tracks are determined by following the centroid of the vorticity maximum associated with the storm circulation. The domain for the centroid calculation is a circular area of three mesh intervals (150 km) radius, centered at the storm location. About 27 grid points fall within the centroid domain. Centroids are computed at each time step. This procedure differs from our previous procedure where only nine grid points were used at 6-h intervals to locate the vorticity maximum. The model track positions vary more smoothly with time using the new algorithm.

The data assimilation procedure determines the least squares fit of the solution of the prediction model to atmospheric data over a specified time interval. Then, this solution is extrapolated forward in time to make a meteorological forecast. When the numerical model is exactly satisfied over the assimilation period, it is a strong constraint. For this case, Φ in (2.1) is identically zero. Derber (1989) introduced a method where the model equations are only approximately satisfied over the assimilation interval. This is the weak constraint and

is accomplished by adding the forcing term Φ to (2.1). The forcing term may be a function of space and time, but for simplicity, Φ will only vary in space for the present study. In this study, assimilation with strong, weak, and combined strong followed by weak or weak followed by strong constraints will be tested over assimilation periods ranging from 6 to 72 h. The input data are winds from objective analyses into which a properly positioned vortex has been inserted. The analyses are available at 6- or 12-h intervals.

The quality of the fit between the atmospheric model and the data is measured by a cost function, which is the sum of squared differences between the atmospheric data and their model counterpart. The cost function can be modified by adding a penalty term that suppresses smaller spatial scales in the solution. This may be desirable when an intense vortex of the scale of a few mesh lengths is present in the data. With this modification the cost function C is given by

$$C = \sum_{n=-N}^{0} \sum_{i=0}^{I} \sum_{j=0}^{J} W_{ij}^{n}(P_{ij}^{n} - \overline{P_{ij}^{n}})^2 + \sum_{i=0}^{I} \sum_{j=0}^{J} \{\sigma[\Delta(P_{ij}^{-N} - \overline{P_{ij}^{-N}})]^2 + \rho[\Delta\Phi_{ij}]^2\}, \quad (2.6)$$

where $\overline{P_{ij}^{n}}$ is the potential vorticity from the objective analyses at the model grid points, P_{ij}^{n} is the potential vorticity from the model, W_{ij}^{n} are arbitrary weights, σ and ρ are specified constants, and Δ is a discretized Laplacian operator defined by

$$\Delta(f_{ij}) = f_{i+1,j} + f_{i-1,j} + f_{i,j+1} + f_{i,j-1} - 4f_{i,j}. \quad (2.7)$$

The subscripts i and j in (2.6) represent x and y indices, n represents the time level, N is the number of time steps in the assimilation period, and I and J are the number of mesh intervals in the x and y directions, respectively. The summation over n in the first term on the right side of (2.6) includes only those time levels for which data exist. The spatial summations in (2.6) include the model grid boundaries. Equation (2.7) is valid for the interior of the model domain. The difference formula for the operator is applied only in the direction parallel to the boundary at the boundary points.

The first term on the right side of (2.6) measures the lack of fit between the potential vorticity of the model and the analyses. The second term is applied only at the initial time ($n = -N$) and penalizes small-scale roughness of the potential vorticity (strong constraints, $\rho = 0$), or the forcing function (weak constraints, $\sigma = 0$). The strength of the filtering is controlled by the parameters σ and ρ. Additional details concerning the cost function and the penalty term are given in DJ93.

The model potential vorticity solution that minimizes the cost function (2.6) is found by systematically varying the initial state potential vorticity P_{ij}^{-N} for the strong constraint. For the weak constraint, the forcing term Φ is varied to fit the model potential vorticity to the data over the assimilation period, while the initial state is held fixed. When there are data at the beginning and end of the assimilation period, and nowhere else, and the penalty term is suppressed, Φ depends only on the data at the end of the assimilation period and has the same number of degrees of freedom as these data. In that case, the potential vorticity solution should equal the data at the end of the assimilation period and the subsequent forecast will be the same as the control run with no assimilation. Numerical experiments have confirmed this. The track forecast errors are within a few kilometers of those for the control run. This result also holds when the assimilation begins with the strong constraint and the weak constraint is used to complete the minimization of the cost function.

For the strong constraint, the cost function can be minimized by computing the gradient of the cost function with respect to the initial state potential vorticity and using this gradient to iteratively improve the initial state vorticity with the conjugate gradient algorithm (e.g., Fletcher 1987). The cost function gradient is computed by the method of Lagrange multipliers. The multipliers satisfy the adjoint equations for the discrete version of the forecast model. The forecast model is integrated forward for the assimilation period and the adjoint equations are integrated backward for the same period, at which point the cost function gradient is calculated. The gradient is used to define a descent direction for the conjugate gradient algorithm, which, along with a descent step, determines the correction to the initial state potential vorticity. An optimum step length for the conjugate gradient algorithm is determined by assuming that the cost function is a quadratic function of the step length. To do this, one assumes a trial step and uses the current descent direction to estimate a new cost function. This, together with the past cost function and the descent direction, determine the optimum step with the quadratic assumption. One complete improvement cycle of the initial state potential vorticity requires a backward integration of the adjoint equations followed by two forward integrations of the forecast model. The iteration process is started with one forward model integration and continues until a preset convergence criterion is satisfied. The weak constraint minimization proceeds in a similar manner except that the cost function gradient is with respect to the forcing function Φ and that gradient is a different function of the Lagrange multipliers (Derber 1989). The details for these calculations are more fully discussed in DJ93.

Convergence for the minimization of the cost function in (2.6) depends very much upon the choice of trial step lengths. Based upon experimentation with our 226 datasets, the initial trial steps were set to 0.035 for assimilation periods of 6 and 12 h; 0.01 for 24 h; 0.005 for 36, 48, and 60 h; and 0.002 for 72 h. The step length is nondimensional because the cost function (2.6) has units of potential vorticity squared and the step length

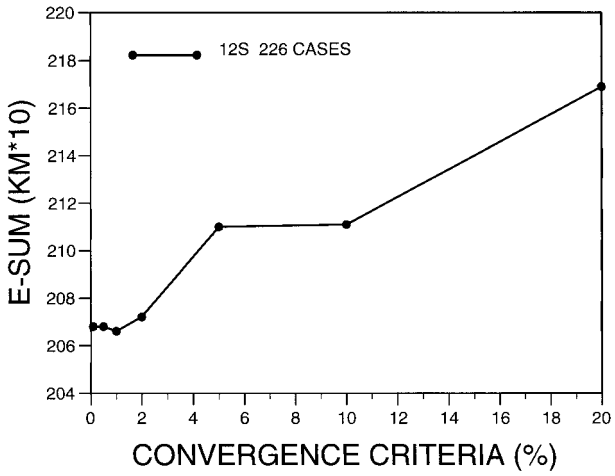

FIG. 1. E-Sum (sum of track forecast errors from 12 to 72 h) for 226 cases and various values of the convergence criteria for the 12-h assimilation with strong constraint (12S) experiment.

is the proportionality constant between the derivative of the cost function with respect to potential vorticity and the potential vorticity adjustment.

A singularity may occur in the equation for the optimum step (see DJ93) due to a poor quadratic fit when both the past cost function and the new cost function from the trial step occur before the minimum in the cost function step length curve. To mitigate this problem, the trial steps are set to 2.0 times the optimum step at the previous iteration. This is a change from DJ93 where 0.8 was used. Sometimes poor choice of the step length results in failure of the conjugate gradient algorithm. This problem becomes worse as the length of the assimilation period increases. Trial and error adjustment of the initial step and the ratio of trial step and past optimum step is used to redefine the step size. These calculations also require about an order of magnitude smaller convergence criteria for the solution of the Helmholtz operators than is necessary for the forward model with no assimilation.

The minimization procedure converges when the cost function decreases by less than 1.0% relative to the previous iteration. Tests were run for 12-h assimilations with the strong constraint (12S) and 12-h data. The results are shown by Fig. 1, where the sum of the mean forecast track errors from 12 to 72 h (E-Sum) are shown for all 226 cases. The value of E-Sum is minimized when the convergence criterion is 1%, although the E-Sum scarcely changes from 0.1% to 1.0%. Other assimilation strategies were also tested with similar results, indicating that the 1% criteria is a reasonable indicator of convergence.

3. Initial data

Datasets for this study consist of 226 individual cases from 17 storms selected from the Atlantic hurricane seasons for 1989–93 (Table 1). In order to qualify for the dataset, the storm must have been classified as a hurricane sometime during its life, had tropical (warm core) characteristics, and there must be enough data for a 24-h assimilation and at least one 72-h forecast.

TABLE 1. Forecast cases for each storm.

Storms	Year	Forecast period (h)					
		12	24	36	48	60	72
Dean	1989	14	13	12	11	10	9
Erin	1989	13	12	11	10	9	8
Felix	1989	11	10	9	8	7	6
Gabrielle	1989	22	21	20	19	18	17
Hugo	1989	20	19	18	17	16	15
Total	1989	80	75	70	65	60	55
Bertha	1990	8	7	6	5	4	3
Gustav	1990	17	16	15	14	13	12
Isidore	1990	22	21	20	19	18	17
Josephine	1990	10	9	8	7	6	5
Klaus	1990	6	5	4	3	2	1
Nana	1990	6	5	4	3	2	1
Total	1990	69	63	57	51	45	39
Bob	1991	6	5	4	3	2	1
Claudette	1991	12	11	10	9	8	7
Total	1991	18	16	14	12	10	8
Andrew	1992	17	16	15	14	13	12
Bonnie	1992	13	12	11	10	9	8
Charley	1992	9	8	7	6	5	4
Total	1992	39	36	33	30	27	24
Emily	1993	20	19	18	17	16	15
Grand total	1989–93	226	209	192	175	158	141

Our model requires winds at each grid point. These data are obtained from analyses that are prepared for an experimental operational barotropic hurricane track model VICBAR (DeMaria et al. 1992; Aberson and DeMaria 1994, hereafter AD94). The analysis levels are 850, 700, 500, 400, 300, and 200 mb. Three domains are analyzed. The synoptic scales are analyzed over an area between 27.5°S and 67.5°N and 140°W and 10°E. The storm environment domain covers a 50° latitude–longitude square area, and the vortex domain extends outward to a radius of 7.2° (800 km), both centered on the current storm location. These analyses are averaged by mass weighting to form a deep layer-mean analysis. This differs from the four-level average used by DJ93. Two upper-tropospheric levels at 300 and 400 mb are added to the mean. These changes, along with modifications to the vortex domain described later, resulted in improved forecasts for the VICBAR hurricane tracking system.

Because there are not enough data to define the hurricane circulation, synthetic data, a symmetric vortex plus straight flow corresponding to the past 12-h motion of the storm, are introduced on the vortex domain. These data are combined with the storm environment and synoptic data in a deep layer-mean spline analysis with four nested grids. In DJ93 the radius of the vortex domain for the synthetic data was only 600 km. This was in-

creased to 800 km to mitigate the problem of misplaced vortices in the background analyses. Several Hurricane Gabrielle (1989) cases (DJ93) showed false currents through the storm center due to the presence of vortex vorticity outside of the old 600-km radius, which is corrected by the new radius. Previously, only the vortex for the storm being tracked was inserted into the analysis. In the new analysis, synthetic vortices are added for each tropical cyclone that is present over the analysis region. The strength and areal distribution of vortex winds are estimated from parameters furnished by the National Hurricane Center (NHC) at the time of the ocurrance of these storms.

In summary, the *new* data are derived from six analysis levels and have synthetic data inserted over a domain of 800-km radius for each storm that is present, while the *old* data are from four analysis levels and have synthetic data inserted over a 600-km domain for just one storm.

The mesh structure for the VICBAR analysis is given by AD94. The nodal spacing and filter wavelengths increase outward by a factor of 2 between the four grids. The filters are part of the cubic-spline analysis algorithm described by Lord and Franklin (1987). The filter wavelengths give an estimate of the smallest horizontal scales that are resolved by the analysis. For the present study, only the outer three nested grids are used to provide initial data to the assimilation model. The finest analysis mesh used here has nodal spacing of 1.2° latitude and filter wavelength of 4.8° latitude, consistent with the original model mesh interval of 100 km (0.9° latitude). The 100-km mesh was sufficient to prevent aliasing at azimuthal wavenumber four in the vorticity on the otherwise symmetric vortex that occurs, if the inner VICBAR mesh is used. However, recent studies showed that the vortex track speeds were slowed by computational dispersion on the 100-km mesh so that the mesh length is now 50 km.

Data from the VICBAR analyses are available at 0000 and 1200 UTC. VICBAR forecasts are also produced at 0600 and 1800 UTC. The initial conditions for these additional VICBAR runs are prepared by combining flow fields from a 6-h VICBAR forecast with a new synthetic vortex that is positioned at the observed storm location as given by NHC (AD94). Because no new data are used in the storm environment, 72-h control forecasts beginning at 0600 and 1800 UTC are not as good as those from 0000 and 1200 UTC. The 0600 and 1800 UTC analyses were intended to provide a 6-h data interval for assimilation experiments. However, when it became apparent that model-fitting forecast tracks could be improved by having the track fit centered at the latest synoptic time, these data became end points for the assimilations at 0000 and 1200 UTC that are discussed in section 6.

4. Hurricane Hugo

DJ93 showed that a 12-h assimilation with the strong constraint (12S) reduced the average Hugo forecast track errors out to 48 h compared to the control forecasts. To relate the current results to DJ93, control forecasts and 12S assimilations were run for Hugo with the current model with both the old and new data. The strong constraint followed by weak (12SW) was also run. Table 2 summarizes the track errors together with direction and speed errors. All are averages that apply to 12-h intervals. The direction errors are the average absolute values of the direction differences between the forecast and the best track directions. The speed bias for individual cases is the ratio of the forecast track speed to the best track speed. The average speed bias is found by weighting each case by the best track speed, in order to avoid a fast bias.

Table 2 shows that, just like DJ93, the 12S 4L track forecasts have smaller errors than the control (CON 4L), but this time extending to 60 h. The forecasts for 12SW 4L are the best for Hugo and show that two time level weak constraint forecasts can be far better than the control, in some cases. The control forecast for the new data (CON 6L), on the other hand, has smaller track errors everywhere than either the 12S 6L or 12SW 6L experiments. Also, note that the control forecasts with the new data have smaller track errors than those with the old data, while the model-fitting forecasts have larger errors.

These results (Table 2) can be understood by reference to the track speed biases. The direction errors give little understanding, because they are fairly small and because they sometimes favor the wrong experiment (note the control experiments).

The track speed biases, on the other hand, give a clear picture of the best experiments. The track speed biases for the CON 4L experiment average about 90%, while the average for the CON 6L experiment is 100%. Clearly CON 6L has smaller track errors, because the speeds are nearest the best track, while the direction error differences are small enough to ignore. The improved track speeds may be due to the inclusion in the wind analysis of two more upper-troposphere levels, where the wind speed is greater, or due to making the initial motion vector more effective by nearly doubling the domain over which it is applied.

Before and after comparison of the assimilation period track speeds for the 12S 4L experiment shows that slow track speed biases are corrected from 85% to 97%. This results in forecast track speeds that are near the best track speeds, which explains the smaller track errors compared with the control. The 12SW 4L experiment is similar, but here slighly smaller direction errors compared with the 12S 4L experiment give track errors that are smaller than both the control and the 12S 4L runs. For the new data, on the other hand, both the 12S 6L and 12SW 6L experiments show track speed biases that are corrected from 94% to 98%. But, due to about 10% acceleration of these speeds during the first 24 h of the forecast, the resulting track speeds become too large and the track errors are greater than the control. This

TABLE 2. Mean forecast track errors (km) for Hurricane Hugo with the old (4L) data and the new (6L) data for the control experiments (CON) and the 12-h assimilations with strong (12S) and strong and weak (12SW) constraints. The average speed bias (%) and the average absolute value of the direction error (°) are given, both measured in 12-h segments with regard to the best track. E-Sum is the sum of the track errors from 12 through 72 h. The BT speed is the average best track speed (m s^{-1}).

	Forecast period (h)							
Experiment	0	12	24	36	48	60	72	E-Sum
1) CON 4L	16	57	98	138	186	245	291	1015
Speed bias		84	91	92	91	87	85	
Dir. error		6	7	8	11	13	15	
2) 12S 4L	14	41	78	104	152	215	298	888
Speed bias	97	98	100	100	98	93	87	
Dir. error	2	4	7	8	11	13	15	
3) 12SW 4L	15	43	77	102	144	190	255	811
Speed bias	97	95	98	97	95	90	85	
Dir. error	2	5	6	6	9	12	14	
4) CON 6L	16	50	88	121	157	204	261	881
Speed bias		94	101	103	102	101	99	
Dir. error		6	8	9	10	13	16	
5) 12S 6L	14	51	97	135	184	227	285	978
Speed bias	98	104	108	109	108	106	101	
Dir. error	2	6	7	9	11	13	14	
6) 12SW 6L	14	53	104	142	178	215	247	939
Speed bias	98	103	108	109	108	105	101	
Dir. error	2	6	8	8	10	11	14	
BT speed	6.6	6.8	6.7	6.6	6.6	6.6	6.5	
Cases	19	19	18	17	16	15	14	

acceleration is present in both control forecasts, but curiously reduced in the 12S 4L or 12SW 4L forecasts. It is also present in the VICBAR forecasts for these data (S. Aberson 1998, personal communication) where the 12-h average track speed increases by 0.7 m s^{-1} between 12 and 24 h. The acceleration seems characteristic of the deep layer-mean analyses for Hurricane Hugo. It may be noted that the track directions are corrected from 6° to 2° during assimilation for both old and new data.

The change of the model mesh from 100 to 50 km revealed a spurious track speed acceleration on the 100-km mesh. This is noted by the control forecasts where the initial track speeds are about 10% slower on the 100-km mesh, due to computational dispersion, while the track speeds are about the same on both meshes from 36 to 72 h. Thus, the correction of the computational dispersion not only improved the initial track speeds, but also corrected a spurious acceleration (being in addition to the acceleration observed for the VICBAR model results) that is present in the first 36 h of the 100-km forecasts.

The results given here show that, even though computational dispersion was present, the good forecasts for Hugo that were reported by DJ93 are correct. For the old data, slow speed biases throughout the control forecast creates the opportunity to improve track forecasts by model fitting. For the new data, however, the model-fitting forecasts for Hugo are worse than the control, due to the correction of slow speed biases for the old data by inclusion of additional wind data from the upper troposphere and by increasing the influence of the initial motion vector.

5. Results: 1989–93

A number of model-fitting issues are examined below by means of our large dataset. They are 1) the length of the assimilation period, 2) testing of various assimilation strategies, 3) role of speed biases and direction errors in understanding track errors, 4) stratification of track errors by storm strength as in hurricanes versus tropical storms, and 5) role of domain size in improving model-fitting forecasts.

The effect of the length of the assimilation period upon track forecast errors is shown by Fig. 2. Here mean track errors are displayed for strong constraints for assimilation periods from 12 to 72 h along with the control experiment errors. There are 157 72-h assimilations for this dataset and these cases are shown with decreasing numbers of cases for forecast times after 12 h. One case (Hurricane Isidore at 1200 UTC on 8 September 1990) failed to converge for the 72-h assimilation (the only uncorrectable optimization failure in the entire set of calculations given in this paper). Track errors increase as the assimilation period increases. This is probably due to greater difficulty fitting a single solution for the barotropic model to increasing numbers of track points. The mean track errors are a minimum about 12 h before the end of the assimilation period, and increase noticeably at the end of this period, but remain less than 100

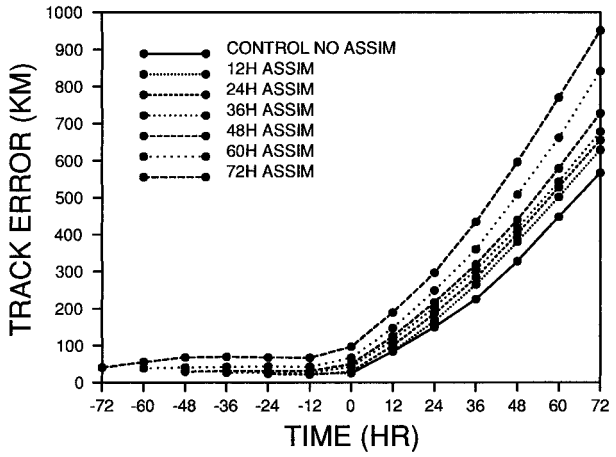

FIG. 2. The average track errors for assimilation periods from 12 to 72 h (157 cases for 12-h forecasts to 82 cases for 72-h forecasts) with the strong constraint and 12-h data plus the control experiment.

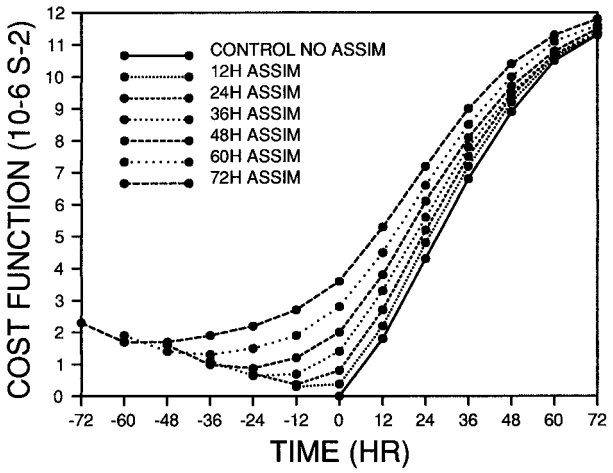

FIG. 3. The average cost functions for assimilation periods from 12 to 72 h (157 cases for 12-h forecasts to 82 cases for 72-h forecasts) with the strong constraint and 12-h data plus the control experiment.

km during all of the assimilation periods. Poorer track fit at the end points is characteristic of a least squares fit and may lead to significant track errors later in an assimilation forecast, in spite of a good fit to data over the assimilation period.

The cost function curves corresponding to Fig. 2 are shown by Fig. 3. Like the track errors, the cost functions increase for all of the forecasts, as the length of the assimilation period increases. The cost function curves fit the data in the middle of the assimilation periods better than at either end, but less well at the end of the period than at the beginning. The results above were created before the change to a 50-km mesh, but would not materially change for that mesh and are the only 100-km calculations reported here. It is shown below that the shortest assimilation period is also favored for a 50-km mesh.

To test various assimilation strategies with the new dataset, 19 experiments were conducted using assimilation periods of 6, 12, and 24 h for the 226 cases of Atlantic tropical cyclones given in Table 1. Tests were run with the strong constraint (S) where the model solution must be exactly satisfied over the assimilation interval and with the weak constraint (W) where the model equations are only approximately satisfied over the assimilation period because of imposed forcing. Mixed constraints consisting of strong followed by weak (SW) or weak followed by strong (WS) were also run. For SW, the strong constraint is applied to convergence (1%) or to 10 assimilation cycles, whichever occurs first, and then the weak constraint is applied to convergence. For WS, 10 assimilation cycles are used for the weak constraint and then strong to convergence. Here convergence for the weak constraint occurs only when three or more datasets are used. When the constraints are switched, the original trial step is restored and a steepest descent step is used to restart the conjugate gradient algorithm. The data intervals for these experiments are 6 or 12 h and the forecasts always begin at 0000 or 1200 UTC.

The experiments are summarized in Table 3 by the mean forecast track errors. The sum of the forecast errors, E-Sum, is used to rank the experiments. These data are homogeneous except for 24S6, 24W6, and 24SW6 where the first Hurricane Isidore case is missing due to the storm having been downgraded to a tropical depression for the first 6-h dataset. Only the 24WS experiment was done to complete the ranking of the constraints, while 24WS6 was omitted, due to excessive optimization failures that occur for the 24-h assimilations with the weak constraint. The 24W and 24W6 experiments have 48 and 63 optimization failures, respectively, that were corrected by trial and error. There are only 15 optimization failures for all of the 6- and 12-h assimilations (about 12 000 cases) that are noted in this paper. These failures are limited to 12-h assimilations beginning with the strong constraint and occur in pairs with one failure occurring nine times due to sensitivity tests for the 12S runs.

Several conclusions may be drawn from the track error summary of Table 3. First, there is no assimilation strategy that gives smaller track errors than the control experiment, except 12W for the 12-h forecast. The best assimilation strategy (smallest E-Sum) is 6W6. Short assimilation periods are favored for each constraint category (S, W, SW, or WS); in fact, for each assimilation strategy the order is 6 h as the best, followed by 12 h, and by the 24-h assimilation period. The order of the constraints for 6- and 12-h assimilation periods is W, WS, SW, and then S. For the 24-h assimilations, the order is SW, W, WS, and S. Only the 24-h assimilations have the same order as DJ93, except for the new WS constraint. Recent results by Zupanski (1997) also show the superiority of the weak constraint with respect to the strong constraint. Apparently the W experiments are

TABLE 3. Summary of mean forecast track errors (km) for 19 assimilation strategies for strong S, weak W, strong followed by weak SW, or weak followed by strong constraints WS. Assimilation periods are 6, 12, or 24 h. Experiment 12S is a 12-h assimilation with strong constraint and 12-h data while 12S6 has 6-h data. The control experiment is CON. E-Sum is the sum of the track errors from 12 through 72 h and ranks these experiments.

	Forecast period (h)							
Experiment	0	12	24	36	48	60	72	E-Sum
CON	26	77	147	230	339	465	616	1874
6W6	25	78	148	233	342	469	621	1892
6WS6	22	79	150	235	344	472	623	1901
6SW6	26	80	151	235	347	473	624	1910
12W	25	76	148	236	348	477	628	1913
12W6	26	79	153	240	349	477	632	1928
12WS6	26	80	154	240	350	478	635	1937
12WS	25	78	152	242	355	484	633	1945
12SW6	25	83	158	247	355	481	634	1957
12SW	26	80	154	247	359	486	635	1961
6S6	25	82	162	253	360	489	645	1992
24SW	28	86	164	258	374	505	649	2037
24SW6	28	88	167	261	373	511	666	2066
12S	26	84	164	261	380	513	664	2066
24W	29	85	166	258	377	513	675	2074
12S6	27	87	168	265	381	513	666	2079
24WS	29	86	167	260	381	519	680	2092
24W6	29	88	168	264	381	521	679	2101
24S	29	93	179	282	404	536	687	2180
24S6	34	99	185	286	401	536	690	2197
Cases	226	226	209	192	175	158	141	

degraded by the strong constraint for the WS experiments. The emergence of W as superior to the SW constraint for 6- and 12-h assimilation periods suggests that problems associated with the vortex scale being near the track displacement during assimilation, which were described in DJ93, may be mitigated by having better grid resolution. The structure of the forcing term Φ for Hurricane Hugo at 1200 UTC on 18 September 1989 is similar to that shown by DJ93 for the 100-km mesh. The mixed SW constraint has about half the amplitude of weak. However, in the present experiments, the amplitudes are all a few percent greater than before, due to faster phase propagation of the vorticity patterns that comes from reducing computational dispersion.

Comparison of experiments with 6- and 12-h data and the same assimilation strategy in Table 3 shows that track forecast errors are usually less for the 12-h data with the 12SW and 12WS experiments being the exceptions. Part of the reason for this may be that the track fit at the beginning of the forecast is always poorer for the 6-h data compared with the corresponding 12-h data assimilation.

The average cost functions for the assimilation forecasts of Table 3 have been compared (not shown) with those of the control forecasts. Only the three best assimilations, 6W6, 6WS6, and 6SW6, have cost functions that are less than the control. Two strategies (12W6 and 12WS6) have smaller cost functions after 12 h and two, 6S6 and 12SW6, are smaller after 24 h, while the remaining experiments are intermitantly better than the control or not at all (24SW). The improved cost functions are only about 1% smaller than the control, which is not enough to ensure smaller forecast track errors for these experiments.

Even though the data in Table 3 show that nearly all of the assimilation forecast errors are greater than the control errors, there are several storms in the sample where the average track errors for some assimilation strategies are smaller than the corresponding control forecasts at all time levels to 72 h. There are 16 such occurrences with Gustav having 9, Charley 3, Bob 2, and Claudette and Klaus having one each. This is out of a total of 323 possibilities (17 storms times 19 strategies). There are 33 cases, including the above, where the first 48-h forecasts have smaller track errors than the control. The nine Gustav forecasts, in order of ascending E-Sums, are 24WS, 12WS, 24W, 12S, 24W6, 6SW6, 24SW, 12W, and 12SW. The Gustav control forecasts have slow speed biases that are capped by 86%, similar to the old Hugo data, but with direction errors (not shown) that are two to three times greater than for Hugo. The 24WS track forecast (not shown) has a 14% smaller E-Sum than the control. Superior speed forecasts account for the smaller track errors to 36 h, while reduced direction errors account for the remaining small errors.

To compare track errors by means of direction error and speed bias, it is useful to consider the growth of the track error of the assimilation forecast with respect to the control over 12-h intervals. This relative track error growth is given by the difference between the error growth (current error minus the past 12-h error) of the assimilation and the control experiment.

Comparing track errors is difficult, because there are

TABLE 4. Mean forecast track errors (km) for the control (CON) and the 12-h assimilation with the strong constraint (12S) experiments. Statistics are measured over 12-h intervals. They are the average speed bias (speed bias, %); the average absolute value of the direction error (dir. error, °); the relative speed bias (rel. spd. bias, %), which is speed bias minus the optimum speed bias (i.e., cosine dir. error); and rel. err. growth (km), which is the growth of the assimilation forecast error (current minus past 12-h error) minus the same quantity for the control forecast. The BT speed is the average best track speed (m s^{-1}). E-Sum is the sum of the track errors from 12 through 72 h.

	Forecast period (h)							
Experiment	0	12	24	36	48	60	72	E-Sum
1) CON	26	77	147	230	339	465	616	1874
Speed bias		90	93	93	93	92	91	
Dir. error		15	23	30	40	48	51	
Rel. spd. bias		−7	1	6	16	25	28	
2) 12S	26	84	164	261	380	513	664	2066
Speed bias	98	99	96	96	96	95	94	
Dir. error	7	18	26	34	41	49	54	
Rel. spd. bias	−1	4	6	13	21	29	35	
Rel. err. growth	0	7	10	14	10	7	0	
BT speed	5.1	5.4	5.4	5.4	5.5	5.6	5.7	
Cases	226	226	209	192	175	158	141	

many forecast tracks with large direction errors. DeMaria et al. (1990) show that if a direction bias exists, track errors are minimized when the speed bias equals the cosine of the direction error so that the projection of the best track along the forecast motion is the same as the forecast motion. Thus, if the direction is in error, track errors are minimized when the forecast is slower than the best track. By considering the difference between the forecast speed bias and the optimum speed bias given by the cosine of the direction error, one may compare experiments. Table 4 summarizes the 12S and CON experiments by the track errors, the speed biases, the optimum speed bias, the direction errors, and the relative growth of the track error of 12S compared to CON by 12-h increments. The idea is that the track errors will grow in one experiment with respect to a second, if the speed biases of the first are farther from the optimum bias than for the second. This assumption should be approximately true for large datasets where initial position errors average out of the track error statistics. For the average of the absolute value of the track direction errors, the contribution to the relative track error growth of Table 4 is estimated from the difference between the track direction errors for the two experiments. Each degree of difference contributes a little less than 4 km of relative error growth per 12-h forecast for a storm moving at 5.4 m s^{-1}, the average track speed for our dataset.

The data of Table 4 show that for the first 12 h the 12S error growth is 7 km greater than the CON error growth. The direction error difference of 3° accounts for about 11 km of error growth of 12S with respect to CON, while the speed biases favor 12S. Somewhat crude estimates of the latter reduce the direction error growth by 2 km giving a net 9-km error growth of 12S over CON. This is in the right neighborhood and shows that the direction errors are more important than the speed errors. For the 12–24-h period and the 24–36-h period, direction error differences of 3° and 4° also dominate the relative track error growth. After 36 h, direction error differences are smaller, except at 72 h, and the speed biases become important in expaining the relative error growth. However, direction errors are dominant through 36 h as the main source of relative track error growth. This result is consistent with data to be given in the next section that shows that model fitting fits the track speed better than direction at the beginning of the forecast. This discussion applies to the 12 worst assimilation strategies of Table 3. However, for the four best strategies, neither direction error nor speed bias account for the larger E-Sums relative to the control. In fact, the E-Sum for 6W6 should be less than the control according to these statistics and this is due to the approximate nature of these calculations that work best for large relative track errors.

Slow average track speed biases are observed throughout the old Hugo control experiment (Table 2). This is also true for the whole dataset, but the relative speed biases for this dataset are mostly fast (Table 4). If one selects only those control cases where the speed bias is slow relative to the best track at all time levels (69 cases), one finds that these track speeds are also slow relative to the optimum speed bias (similar to the old Hugo data). Stratification of the whole dataset in this manner shows that 12 of 16 (24-h assimilations with 6-h data omitted) assimilation strategies have smaller E-Sums (not shown) than the corresponding control forecasts and, in fact, the four best strategies plus 12WS, 12SW, and 24WS of Table 3 have average track errors that are less than the control from 12 through 72 h. The greatest error reduction is about 6% for the 24W run, although these errors are about 14% greater than those for the 226-case dataset (control errors are 34% greater). The greater track errors for this subset of cases are probably related to an observed track speed acceleration from 4.9 to 7.7 m s^{-1} for the first 60 h of these forecasts, which contrasts with the whole dataset where the best track speeds are nearly uniform (Table 4). In most of

these cases the observed acceleration was not matched by the barotropic forecasts for these data. Clearly, slow relative speed bias for the entire control forecast is a situation where variational assimilation can improve hurricane track forecasts. Unfortunately, these biases are only known after the fact.

It is interesting to note that nine Gustav cases belong to the slow bias stratification and that the Gustav control forecasts (17 cases) have slow average relative speed biases with an observed track speed acceleration of just 0.6 m s^{-1} for 60 h. For Gustav, 16 of 19 assimilation track forecast strategies have smaller E-Sums than the control forecast tracks, including all eight experiments with just 12-h data for the assimilation.

Hurricane–tropical storm stratification at $t = 0$ of our data shows a tendency for tropical storms (65 cases) to have larger control forecast errors than for hurricanes (161 cases), but the assimilation strategies are more successful for tropical storms. This result is based upon 10 of the best 12 assimilation strategies of Table 3 having E-Sums (not shown) for tropical storms that are closer to the corresponding control forecasts than is the case for hurricanes. The 6SW6 and 6W6 experiments show tropical storm E-Sums that are, respectively, 2 and 4 km greater than the control while hurricane E-Sums are 50 and 23 km greater, respectively. Tropical storm E-Sums are about 100–200 km larger than hurricane E-Sums. However, this is partly the result of one tropical storm, Josephine, which executed a badly forecast 72-h track loop in the middle of the Atlantic Ocean.

Better assimilation forecasts may be achievable by improving the prediction of the environmental flow fields. This is tested by solving our model on a 96 × 96 mesh interval grid in place of the usual 256 × 160 intervals. The boundaries are now imposed by time interpolation of 12-h analyzed data to simulate improved environmental flow fields. The grid is centered on the storm longitude, but no farther west than 75° nor farther east than 30° (the longitude had to be moved 10° east for three Emily cases to keep the storm on the grid). The center latitude is either 35° or 30°N for storms south of 20°N. This grid system is applied to the control and to 12 assimilation strategies with 6- or 12-h assimilation periods.

The results of these experiments show about 100-km reductions of E-Sums for each experiment (not shown) with the control having the least reduction so that each experiment is closer to the control than are the corresponding results for the 256 × 160 grid. No experiment has smaller E-Sums than the control. However, both the 6W6 and the 6SW6 experiments have E-Sums that are only 2 km greater than the control. Thus, model-fitting forecasts are improved by using a smaller domain with time-dependent boundaries. In addition to saving computer resources, this suggests that improved environment forecasts may improve model-fitting track forecasts.

With the notable exception of Gustav, which fits the same mold as the old Hugo data, the present model-fitting track forecasts are not very good. Examination of the fit of the tracks during assimilation shows that the tracks fit very well at the middle time of the assimilation period, but that when the track fit at the beginning of the forecast is examined, the track fits are not as good. The variational approach generally fits data best in the middle of the interval, so that this is a fundamental problem with the present approach. However, if one uses track positions observed after the beginning of the forecast, a better centered track fit for the track data at the synoptic times (0000 and 1200 UTC) is possible. This result is discussed in the next section.

TABLE 5. Model fit to best track speed and direction for the assimilation period ($t = -6$ h) and the beginning of the forecast ($t = 0$ h) for 12-h assimilations with 6-h data. Statistics are average speed bias (%), absolute value of direction error (°), and E-Sum (km). Experiments like 12WS6 6H have the track positions from 6 h included in an assimilation from $t = -6$ h to $t = 6$ h. Control experiment E-Sums are 1874 and 1695 km for the usual model fit and the assimilations with the 6-h future data, respectively.

	Track error statistics				
Time (h)	−6	0	−6	0	
Experiment	Speed Bias		Dir. Error		E-Sum
12WS6	101	98	9.6	10.2	1937
12WS6 6H		98		7.3	1652
12W6	101	99	9.7	10.7	1928
12W6 6H		98		7.9	1669
12SW6	98	95	8.5	11.1	1957
12SW6 6H		96		7.1	1690
12S6	96	99	7.8	12.2	2079
12S6 6H		96		7.5	1712
Cases	226	226	226	226	

6. Model fitting with future storm positions

The model-fitting experiments for the large dataset discussed in section 5 always have larger E-Sums than the control forecasts. However, it was speculated that the use of future positions for model fitting would give smaller track errors, due to having a centered fit of the model to the observed track at the synoptic times of 0000 and 1200 UTC. At these times, the track fit has already substantially departed from the observed track as is shown by Table 5 where the average track direction errors and speed biases are given for the 12-h assimilation period ($t = -6$ h) and the beginning of the forecast ($t = 0$ h) for the four 12-h assimilations with 6-h data from Table 3. The fit of the model track direction to the best track is 1°–4° poorer at the beginning of the forecast than at the middle of the assimilation period. The track speeds, on the other hand, are often better fit to the best track at $t = 0$ than at $t = -6$ h. The track direction errors seem to control the E-Sums for these experiments.

Track-fit data for the assimilation period and the end of this period were also examined for the 24 assimilations with 6-h data. These data show 4°–6° greater di-

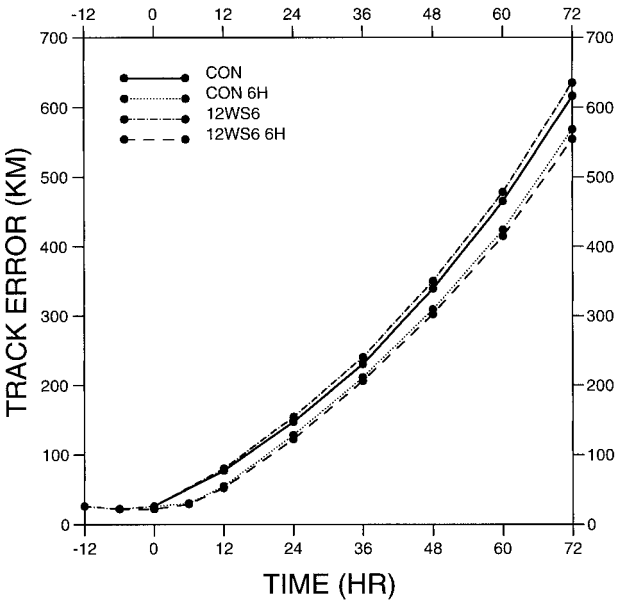

FIG. 4. The average track errors for the control experiment (CON), for the control experiment with the vortex relocated at 6 h (CON 6H), for the 12-h assimilation with weak and strong constraints and 6-h data (12WS6), and for the 12-h assimilation with weak and strong constraints and 6-h data that is centered at $t = 0$ h with initial data from a 6-h forecast with the vortex repositioned (12WS6 6H).

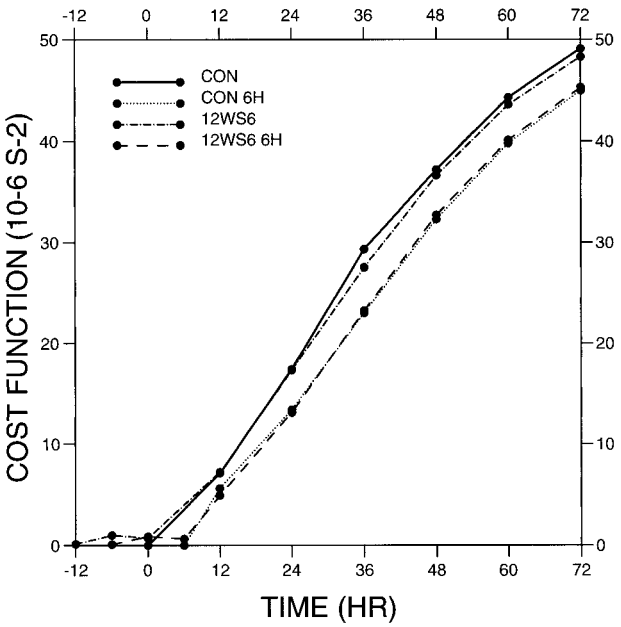

FIG. 5. The average cost functions for the control experiment (CON), for the control experiment with the vortex relocated at 6 h (CON 6H), for the 12-h assimilation with weak and strong constraints and 6-h data (12WS6), and for the 12-h assimilation with weak and strong constraints and 6-h data that is centered at $t = 0$ h with initial data from a 6-h forecast with the vortex repositioned (12WS6 6H).

rection errors at $t = 0$ h compared with the assimilation period. For the 6-h assimilations, track-fit statistics for the best track seem to show that the storm track is best fit at the end of the assimilation period. This is misleading, because the model is fit to the operational track, determined at the time of the storms occurrance, and not to the best track. When the track-fit data are calculated with respect to the operational track, the track fit is, as before, best for the assimilation period compared to the end of this period. For example, Hurricane Josephine, which has the largest track errors for any storm in this sample, has a best track fit of 24° error for the assimilation and 14° at the end of this period, while the operational track fit shows 6° and 11°, respectively. These large differences are due to the differences between the operational track and the best track and the 6-h averaging period. The best track is the correct choice for the calculation of track errors, but track-fit statistics may have to consider the operational track.

In order to have the track fit centered at synoptic times, the 12-h assimilations are run with the assimilation beginning at $t = -6$ h and ending at $t = 6$ h. This is done by using the 0600 and 1800 UTC analyses from VICBAR for the $t = 6$ h data. These data are 6-h forecasts with the vortex repositioned at 6 h by using the observed position from NHC. The data for $t = -6$ h are obtained by making a model fit to the data from $t = -12$ h, $t = -6$ h, and $t = 0$ h with one of the 12a6 (a represents the constraint) experiments and saving the data from $t = -6$ h for input for the centered track-fit experiments. When this is done, the track direction fit at $t = 0$ h is greatly improved as shown by Table 5. These results use the best combinations of $t = -6$ h data and constraints, which are 12WS6, 12W6, 12W6, and 12SW6 for the 12WS6 6H, 12W6 6H, 12SW6 6H, and 12S6 6H experiments (6H refers to the 6-h future data that end the assimilation), respectively. A significant part of the improved track fit at $t = 0$ h is due to the use of assimilated data to begin the assimilation at $t = -6$ h in place of the VICBAR data. The additional improvement is 1° for the 12W6 experiments and occurs because the $t = 0$ h track position is accounted for in both the $t = -6$ and $t = 0$ h data.

The forecast track errors for the 12WS6, 12WS6 6H, and the control (CON) experiments are shown by Fig. 4. The large track error reduction for 12WS6 6H compared to 12WS6 is clearly shown and now 12WS6 6H has track errors that are 12% smaller than the control experiment. Similar large changes in the cost functions for these experiments are shown by Fig. 5. The time coordinate for the 12WS6 6H experiment is the same as 12WS6, even though the real forecast begins at 6 h where the assimilation ends. This seems reasonable, because the only observations from 6 h are the vortex center location and a strength estimate.

The control forecasts can also be stopped at $t = 6$ h and the storm repositioned from NHC data. Again, the 0600 and 1800 UTC VICBAR data are used to continue the control forecasts from $t = 6$ h. The resulting control forecasts now have an E-Sum of 1695 km. Figures 4

and 5 also show the track error and cost function for the control experiment (CON 6H) with the vortex repositioned at $t = 6$ h. The best model-fitting forecast 12WS6 6H now has 2.5% smaller track errors than CON 6H and the errors are smaller at each time level from 12 to 72 h. The cost functions for the 6H experiments are both less than for the original control, but the 12WS6 6H cost function is smaller than that of the CON 6H only at 12 and 24 h.

The E-Sums for the 12WS6 6H experiments are 1652, 1653, 1654, and 1655 km for data at $t = -6$ h that are prepared by the 12WS6, 12S6, 12SW6, and 12W6 experiments, respectively. The WS constraint is superior to W when assimilated data and future data are used to begin and end the assimilation, while the reverse is true when only past and current analyses are used (Table 3). The W constraint modifies the barotropic model over the assimilation period by fitting the model most closely to the end of the dataset (see Fig. 5) without changing the initial state vorticity. The WS constraint improves the assimilation track fit by making small adjustments to the initial vorticity, while using the modified barotropic model.

In order to further see how preparation of the data for the beginning of an assimilation by an earlier assimilation changes track errors, the experiments with 6-h assimilation periods that are summarized by Table 3 were rerun, beginning the assimilation with the assimilated data that are used to begin the 12W6 6H experiment. The E-Sums for 6W6, 6WS6, 6SW6, and 6S6 are reduced by 6, 18, 22, and 56 km, respectively, but none are less than the control. These track error reductions show error improvement at each time level from 12 to 72 h. This occurs because these assimilations start with data that account for the data at $t = 0$ h.

The 6H experiments described here use 6-h future track positions. Thus, these results might appear to have little operational utility. The operational hurricane track models at NHC are run at about 1 h after synoptic time, so a current synoptic time analysis is not available. However, center fixes from satellite and aircraft are typically available at the current synoptic time. Thus, the information available to the track models are analyses at 6-h intervals, the most current of which is 6 h old, and track positions at 6-h intervals all the way up to the current synoptic time. This information is the same as that used in the 6H experiments. The results given here certainly show that this proceedure warrants serious consideration.

Because model fitting requires far greater use of computer resources than is required to modify the control experiment with a future track position, the present recommendation is to use the modified control experiment to improve operational hurricane track forecasts. However, the 2.5% further track error reduction obtained with the present variational model may be worth consideration in the future. Leslie et al. (1998) have shown that high quality satellite winds may be assimilated with the three-dimensional version of the generalized inverse model of Bennett et al. (1993) and give improved hurricane track forecasts. A combination of our strategy and satellite winds may give even better track forecasts than reported here.

7. Summary and conclusions

The customary approach of model fitting fits the model to past and present observations to make a forecast into the future. When this approach is applied to the hurricane tracking problem, the track fit to the observed storm positions is best somewhere in the past and may not be very good by the beginning of the forecast. With the current barotropic model and the 226-case dataset, this leads to assimilation track forecasts that on average always have greater track errors than the control forecast, which uses only the current data without assimilation. If one introduces a track position a little way into the future (here 6 h), a centered track fit for the model to the observed track is obtained in which the track direction difference from the observed track at the beginning of the forecast (time $t = 0$ h) is reduced by several degrees compared with the assimilation with past and present data only. For the present experiments, the $t = 6$ h data come from a 6-h VICBAR forecast, with the storm repositioned at 6 h using the observed position from NHC. The $t = -6$ h data are obtained from 12-h assimilations between $t = -12$ h and $t = 0$ h. The best model-fit forecast is 12WS6 6H, which has an E-Sum of 1652 km compared with 1874 km for the control forecast. If the control forecast is also modified by repositioning the vortex at 6 h in the manner done for the model-fitting experiment, then the modified control forecasts have an E-Sum of 1695 km. Thus, the addition of the 6-h future track position into both the assimilation and control forecasts results in model-fitting forecasts that have 2.5% smaller E-Sums than the comparable control forecasts. The assimilation track errors are also smaller at all time levels from 12 to 72 h. This method has application to operational forecasting, since the most recent analysis available is 6 h old at the time the NHC track models are run, but current center positions are available.

The model-fitting strategy that gives the smallest forecast track errors when only past and present data are used is the weak constraint. However, when a future track position is included in the assimilation by means of a short forecast and repositioning of the vortex to the observed position, the best constraint is a combination of weak followed by strong. Generally, short assimilation periods are favored for all constraints. For 6- and 12-h assimilation periods with past and current data, the order of the constraints by increasing track errors (E-Sum) is W, WS, SW, and S. With the future track positions, the first two strategies exchange places. The 24-h assimilations have too many optimization failures to be practical (ranging from 6% to 28%), while these

failures are extremely rare at the shorter periods (no failures for assimilations that begin with the weak constraint or for 6-h assimilation periods).

This manuscript deals primarily with averages for the 226 cases. Smaller samples show considerable variability in the forecast track errors. This is shown here for Hurricane Gustav and the stratification by slow track speeds for 69 control cases where 24-h assimilations have the smallest E-Sums, in spite of their low ranking for the whole dataset.

Two conclusions are drawn from the experiments reported here. First, hurricane track forecasting by the present assimilation model improves forecasts beyond the corresponding control forecast only when future track positions are included in the assimilation. The use of future track positions makes it possible to take advantage of the better variational track fit at the middle of the assimilation period, by placing the center of the assimilation period at $t = 0$ h. Second, because the control forecast with vortex repositioning is nearly as good as the corresponding model-fitting track forecasts, one may choose to reposition the vortex during the control forecast, rather than implement the far more expensive model-fitting solution. A 10% average reduction of track errors seems possible in this manner. Of course, operational considerations of timeliness of the forecast tracks may dictate the details for including future track positions in operational models. A fringe benefit of using future observed positions in a forecast is that a better track point at $t = 0$ h may be included in the process. This would be useful when small timescale oscillations are observed in the track or when clouds interfere with satellite fixes.

Acknowledgments. The authors thank Hugh Willoughby, Lloyd Shapiro, and an anonymous reviewer for comments on an earlier version of the manuscript. John Festa and the Physical Oceanography Division at AOML provided computer support.

REFERENCES

Aberson, S. D., and M. DeMaria, 1994: Verification of a nested barotropic hurricane track forecast model (VICBAR). *Mon. Wea. Rev.,* **122,** 2804–2815.

Bennett, A. F., L. M. Leslie, C. R. Hagelberg, and P. E. Powers, 1993: Tropical cyclone prediction using a barotropic model initialized by a generalized inverse method. *Mon. Wea. Rev.,* **121,** 1714–1729.

Cressmen, G. P., 1958: Barotropic divergence and very long atmospheric waves. *Mon. Wea. Rev.,* **86,** 293–297.

DeMaria, M., and R. W. Jones, 1993: Optimization of a hurricane track forecast model with the adjoint model equations. *Mon. Wea. Rev.,* **121,** 1730–1745.

——, M. B. Lawrence, and J. T. Kroll, 1990: An error analysis of Atlantic tropical cyclone track guidance models. *Wea. Forecasting,* **5,** 47–61.

——, S. D. Aberson, K. V. Ooyama, and S. J. Lord, 1992: A nested spectral model for hurricane track forecasting. *Mon. Wea. Rev.,* **120,** 1628–1643.

Derber, J. C., 1989: A variational continuous assimilation technique. *Mon. Wea. Rev.,* **117,** 2437–2446.

Fletcher, R., 1987: *Practical Methods of Optimization.* John Wiley and Sons, 436 pp.

Leslie, L. M., J. F. LeMarshall, R. P. Morison, C. Spinoso, R. J. Purser, N. Pescod, and R. Seecamp, 1998: Improved hurricane track forecasting from continuous assimilation of high quality satellite wind data. *Mon. Wea. Rev.,* **126,** 1248–1257.

Lord, S. J., and J. L. Franklin, 1987: The environment of Hurricane Debby (1982). Part I: Winds. *Mon. Wea. Rev.,* **115,** 2760–2780.

Zupanski, D., 1997: A general weak constraint applicable to operational 4DVAR data assimilation systems. *Mon. Wea. Rev.,* **125,** 2274–2292.